

MAE 222: Mechanics of Fluids

Lift and Drag Effects of a Rear Wing on a Passenger Vehicle

Fall 1997 Independent Lab Project



**Harris Yong with Randy Chang
January 13, 1998**

Abstract

This experiment explored the lift and drag effects of a rear wing mounted on a performance vehicle model, with wind speed ranging from 30 mph to 90 mph. Results were largely consistent with expectations—there was noticeable downforce, especially at higher speeds and at a spoiler height to chordlength ratio of around 1.0 to 1.3. There was also a measurable, but minute, increase in drag associated with increased downforce. However, further testing is required to validate the data obtained from the small 1/18 scale model.

Introduction

The study of aerodynamics is an increasingly important aspect of vehicle design. It is estimated that aerodynamic drag is the dominant form of resistance for vehicles cruising at speeds of 50 mph (80 km/h) or greater, and thus the fine tuning of aerodynamics can lead to significant decreases in fuel consumption and overall efficiency. Also important in road vehicle design is the concept of aerodynamic lift, where pressure differences lift the vehicle and reduce its downward normal force, thereby jeopardizing stability and traction at high speeds.

A very wide range of factors affect aerodynamics. The factors of vehicle drag, for instance can be looked at in terms of frictional drag and pressure drag, where the former is associated with the interface of the vehicle and the air, and the latter is associated with the pressure gradients, wakes and eddies (Smits 318-19). Since, for road vehicles, the most significant factors are external flow this lab project will be discussing aerodynamic drag in terms of these factors. In other words, this project will treat vehicles as relatively bluff bodies. As such, by far the greatest contribution to drag is in the afterbody, where the separated flow can cause a very adverse pressure gradient.

Aerodynamic lift, the force that causes a vehicle's normal force on the ground to reduce as speed increase, is also important, especially at high speeds, as available traction from the tires can be adversely affected. Again a primary contributor is the existence of pressure gradients. In very simple terms, the flow over a vehicle's body is lower in pressure than that underneath due to the vehicle's shape and the longer path of travel over the vehicle top, thereby producing an upward, destabilizing force to the vehicle.

In light of these difficulties in design, automobile manufacturers have experimented with many various ways of combating drag and lift, including experimenting with shapes like the teardrop shape of the GM's EV1 electric vehicle, as well as the smoothening of underbodies. However, this project will look at the effects of add on wings, which seem to be popular in racing and the aftermarket crowd and are often not integrated into passenger vehicle production except for high performance models.

Although studies tend to show that a front spoiler mounted close to the ground tends to improve aerodynamics better than a rear spoiler mounted at the trailing edge (Bearman 109), rear mounted add-on aerodynamics, especially wings are by far more popular. Although there is no doubt that a rear spoiler or wing can enhance aesthetics, we would like to see whether the advertising claims of reducing lift and/or drag is warranted.

Definitions

Although the word "spoiler" is often used generically to describe aerodynamic add-ons to the rear of a vehicle, a wing is specifically an elevated foil, in the shape of an inverted airplane wing, with clearance for the passage of air between it and the car body. This experiment will be testing the effects of the wing, although a spoiler that is attached to the car rear with no clearance for air has some similar characteristics.

Aerodynamic resistance (with the dimensions of force) can be defined as shown in Equation 1, where ρ is the density of air, C_D is the coefficient of drag, A_f is the frontal area of the vehicle, and V_r is the speed of the vehicle relative to the wind.

$$F_{drag} = \frac{\rho}{2} C_D A_f V_r^2$$

Equation 1: Drag force definition

Because the non-dimensionalized C_D is most useful in vehicle to vehicle

comparison, this is the most frequently published value, and is defined in Equations 3 and 4. The frontal

area, A_f , is literally the area that is projected by a beam of light, with the angle of incidence parallel to the central longitudinal axis of the vehicle. Because this is difficult to obtain and calculate, the formula shown, based on data collected for passenger cars from 800-2000 kg in mass is

$$A_f = 1.6 + 0.00056(m_v - 765)$$

Equation 2: Frontal area approximation.

fairly accurate, where A_f is in m^2 and m_v is the mass of the vehicle in kg. Equation 2 shows the approximation.

The non-dimensional coefficient of lift, C_L and C_D , the coefficient of drag, can be defined as shown in Equations 3 and 4, respectively. They are a rearrangement of Equation 1. These non-dimensional parameters allow one to extrapolate aerodynamic forces on larger, real vehicles.

$$C_L = \frac{F_{lift}}{\frac{1}{2} \rho V_r^2 A_f}$$

Equation 3: Definition of lift coefficient.

$$C_D = \frac{F_{drag}}{\frac{1}{2} \rho V_r^2 A_f}$$

Equation 4: Definition of drag coefficient.

The Theory Behind Rear Spoilers

"The purpose of spoilers, by definition, is to modify the airflow around the car..." (Scibor-Rylski 84). In the most general terms, one can see the function of a rear wing as an inverted airplane wing mounted at the downstream end of an ellipsoid. Smoke tunnel results show that the addition of the spoiler/wing increases the lower base pressure of the ellipsoid and accelerates the flow, generating downforce, explaining the decreased lift (Katz 226). Scibor-Rylski explains that the role of the spoiler tends to break-up the smooth flow over the top of the vehicle, slowing it down so that the pressure over the top of the

vehicle is increased, decreasing the undesirable lift (84). However, the actual effectiveness is very dependent on many factors, one of which is the spoiler's height, chordlength (front to back) and length (wingspan).

For drag, a well designed rear spoiler may induce beneficial turbulent flow because turbulence is more resistant to flow separation (Smits 320), thereby reducing the low pressure wakes behind a vehicle. Again, with the ellipsoid and inverted wing model, the higher speed flow created near the wing is the cause for turbulent flow. As a result, the wing can reattach the flow partially and reduce the area of flow separation (Katz 226).

In tests performed by Hucho a solid rear trailing edge spoiler (not a wing) was placed perpendicularly on a model with a rounded rear. By varying the amount of protrusion, Hucho was able to reduce the model's C_D from about 0.38 to a minimum of 0.33, while the C_L over the rear axle decreased from 0.28 to 0.14 (35). The optimal protrusion in light of lift and of drag was at 60 mm, a rather conservative size.

One should note that Hucho's data shows that a rear spoiler seems more effective in reducing lift than drag, and we will see if this is true for wings as well. Hucho also mentions that this preferential improvement on lift does not only apply to rear spoilers. Less extensive tests show that even with front and fender spoilers, lift seems to be affected the most, and this is reflected in real vehicles as well. The Viper GTS actually comes with an integrated rear spoiler—an increase in height at the trailing edge of the rear deck. In the FIA Supertouring BMW M3, an extension of the front spoiler and the addition of a rear spoiler, brings the coefficient of drag down minutely (from 0.31 to 0.30), but rear lift is reduced by 0.12 (from 0.126 to 0.006) (Katz 17). In fact, in generating downforce to counteract lift, many spoilers increase drag slightly.

The spoiler height, a parameter in our experiment also appears to be a significant factor, according to Katz. For a raised spoiler (i.e., with a gap for airflow underneath the spoiler), the best height to chordlength ratio is about one (228). An apparent phenomenon is that at height to chordlength ratios lower than about 0.5, the spoiler loses its effectiveness, due to fact that the gap between the car and spoiler is only wide enough for the boundary layer (Katz 228). We do not expect that this will pose a problem with our experiment as we will not be testing extremely low spoiler heights.

As aforementioned, front spoilers tend to be more effective than rear spoilers as they do not only change the pressures at the rear of the vehicle but also at the underbody and the front. Hucho explains that a front spoiler is effective because, in redirecting the flow that would have passed beneath the vehicle, there is a drop in underbody pressure (decreasing lift) and underbody velocity (decreasing frictional drag) (33).

Figure 1 below show the coefficient of pressure, C_p , at various points of a bluff body that can be used to approximate a vehicle. Notice that a rear spoiler increases the C_p at the trailing edge where as a front bottom

leading edge spoiler reduces the pressure underneath the vehicle body. Figure 2 shows how a wing's dimensional ratios affects its reducing lift and drag coefficients. As aforementioned, it seems that the best ratio of the height to chordlength is approximately one.

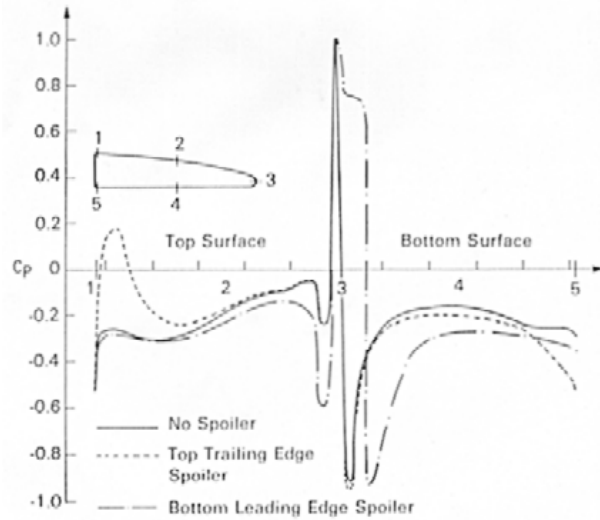


Figure 1: Pressure distributions for a car like body (Bearman 111).

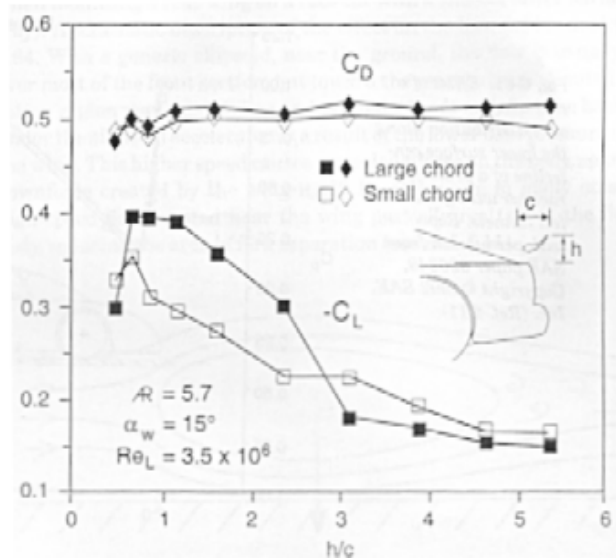


Figure 2: Wing effects based on the height vs. chordlength ratio (Katz 228).

Experiment

Please note that, in the body of this report, errors are not indicated, other than for important aerodynamic data. They are given in the data sheet in the appendix (Table 2).

In order to test the effects of a rear wing, we obtained a Dodge Viper GTS model with a scale of 1/18. For the spoiler, we used balsa wood that came shaped as a foil and wrapped with tape. The size of this wing is a little large relative to the model (the model was about 24.7 cm long, while the chordlength and length of the wing were 2.55 and 10 cm, respectively). Still, we were quite confident that we can still extrapolate the effects of a true wing. Drilling vertically through the rear quarter panels of the model, we were able to mount the spoiler on with screws, which makes the setup height adjustable. We decided against testing effects of spoiler angle as the thin foil made it difficult to mount the spoiler at different angles without damaging the fragile balsa wood. Please see the figures for more information.

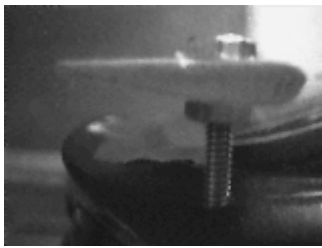


Figure 3: Side view of spoiler and attachment design.



Figure 4: Side view of vehicle rear.



Figure 5: Side view of model mounted on sting.



Figure 6: Front view.



Figure 7: Rear view.



Figure 8: Rear 3/4 view.

In order to obtain measurements of aerodynamic forces, the spare tire under the rear hatch was removed and a hole drilled through the licence plate area in order to allow the insertion of a screw, which was attached to a tube mounted on the sting of a wind tunnel, with speeds varying from 30 mph to 90 mph, roughly reflecting the North American city to highway speed range (30, 50, 60, 70 and 90 mph). At these speeds, the Reynolds numbers of the model car (based on overall length) ranged from $2.2 \text{ E}5$ to $6.5 \text{ E}6$, which is lower than the real car's Reynolds numbers of $4 \text{ E}6$ to $1 \text{ E}7$. This may cause some errors, discussed later. The Re for the wing, based on chordlength, ranged from $2.2 \text{ E}4$ to $6.7 \text{ E}4$.

Published data showed that the real Viper has a C_D of 0.35, and we obtained the approximate frontal area from the equation defined earlier, using the vehicle's published mass of 1550 kg, and dividing this true frontal area by the square of the scale (i.e., $1/18^2$) to attain the model's frontal area of 0.00630 m^2 (See Equation 8 in the appendix). We estimated an error of 15%.

Because it is estimated that open windows increase the drag coefficient--anywhere from 5% as Wong states (183) to 10% (Katz 223)--we taped the windows shut. Because of the known affects of ground clearance on lift and drag, we were able to place a fake floor (not moving, unfortunately) just below the Viper model, and stuck some soft foam between the wheels and the floor. The reasons for this interface, and the effects of the floor will be speculated in the discussion section.

$$\begin{aligned} 1F_{Normal_N} &= 0.0037F_{Normal_{counts}} \\ 1F_{Axial_N} &= 0.00218F_{Axial_{counts}} \\ F_{Axial} &= Weight \cdot \sin \theta \end{aligned}$$

Equation 5 & 6: Sting calibration.

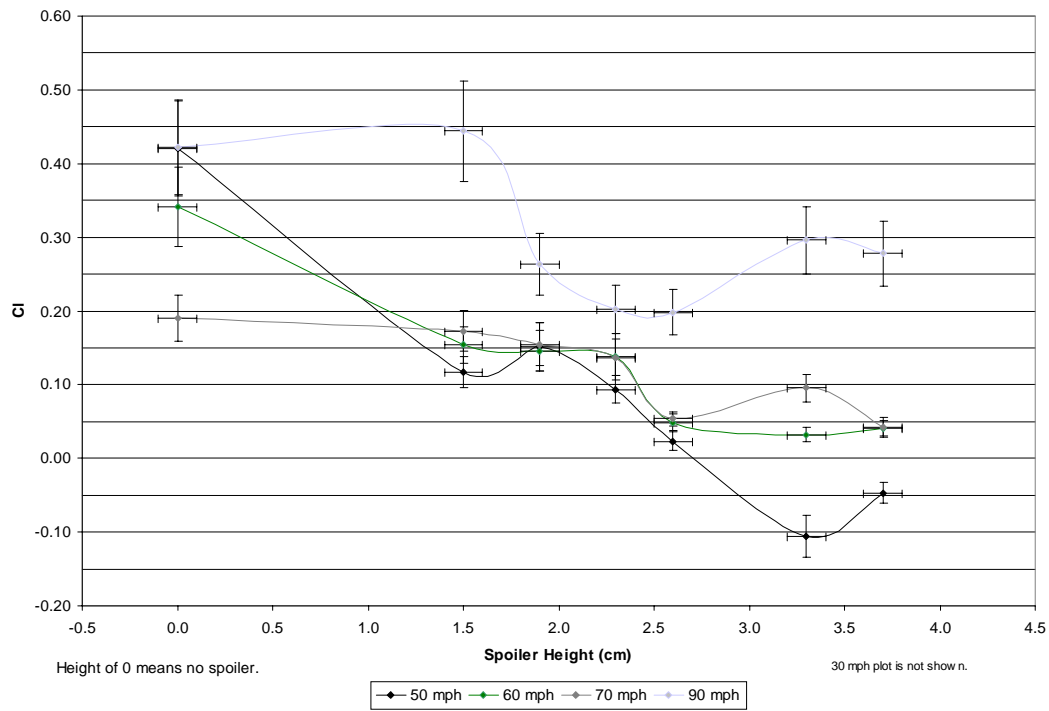
The sting must be calibrated so that meaningful units such as N can be obtained from the apparatus' arbitrary counts. For the normal force relation, we hung weights with masses of 20, 50, 100, 200, and 500 g. Taking the 0 mass point into consideration and also forcing the y-intercept of the graph of Newtons vs. counts, we obtained the following conversion ratio shown in Equation 5. In order to get the axial conversion, we hung the same weights at 15° and used the relation shown in Equation 5 to determine the actual axial force imparted on the sting. The conversion is shown on the left, together with the conversion for the normal force. The sting calibration chart is shown as Figure 20, in the appendix. The normal and axial force readings can then be taken at the prescribed speeds. Since the angle of attack is at 0°, the normal and axial force readings can be translated directly into lift and drag (with a sign change for lift) (Equation 6). There is some doubt as to whether the normal force measures lift as defined by the automotive industry, and this will be discussed later.

Results

Table 1: Important aerodynamic values based on spoiler height.

	Speed (mph)	30	50	60	70	90	Avg.
	Re(Models)	2.2 E5	3.6 E5	4.3 E5	5.0 E5	6.5 E5	4.32E5
 <p>Figure 9: No spoiler. h/c = 0.</p>	C_L	0.88	0.42	0.34	0.19	0.42	0.45
	C_D	0.53	0.40	0.39	0.37	0.36	0.41
 <p>Figure 10: Height = 1.5 cm. h/c = 0.6</p>	C_L	-0.03	0.12	0.15	0.17	0.44	0.17
	C_D	0.47	0.4	0.42	0.40	0.39	0.42
 <p>Figure 11: Height = 1.9 cm. h/c = 0.7</p>	C_L	0.10	0.15	0.5	0.16	0.26	0.16
	C_D	0.51	0.42	0.42	0.42	0.41	0.44
 <p>Figure 12: Height = 2.3 cm. h/c = 0.9.</p>	C_L	0.13	0.09	0.14	0.14	0.20	0.14
	C_D	0.45	0.42	0.45	0.44	0.43	0.44
 <p>Figure 13: Height = 2.6 cm. h/c = 1.0.</p>	C_L	-0.19	0.02	0.05	0.05	0.20	0.03
	C_D	0.55	0.44	0.43	0.44	0.42	0.45
 <p>Figure 14: Height = 3.3 cm. h/c = 1.3.</p>	C_L	-0.45	-0.11	0.03	0.10	0.30	-0.03
	C_D	0.51	0.44	0.45	0.45	0.43	0.46
 <p>Figure 15: Height = 3.7 cm h/c = 1.5.</p>	C_L	-0.26	-0.05	0.04	0.04	0.28	0.01
	C_D	0.52	0.43	0.45	0.44	0.42	0.45

Cl vs. Spoiler Height



Cd vs. Spoiler Height

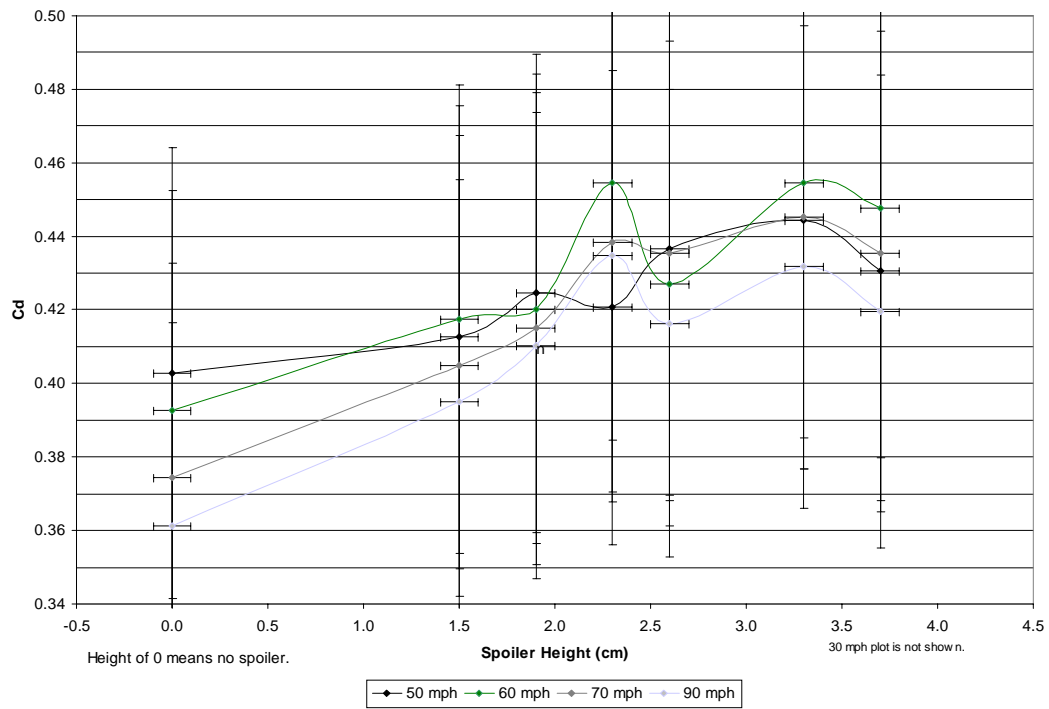


Figure 16 & 17: Cl and Cd vs. Spoiler Height.

In general, the results are largely consistent with expectations: a rear mounted wing does

decrease lift at the slight expense of drag. Furthermore, a wing does seem to become more efficient in producing downforce as height increases because drag does not increase as quickly as lift.

First of all, I did not include the 30 mph graphs as the low speed meant high relative errors. Further factors affecting its accuracy such as transitional flow is discussed later.

We noticed that, despite the drag and lift coefficients being normalized for speed variation, there is a distinct trend of both values decreasing with speed (with all other variables held constant). An explanation for this is given later in the discussion section. The exception is that the lift coefficient increased significantly at 90 mph. But as a result, I will be primarily quoting coefficients averaged over the tested speeds. More data is available in Table 1 and in the appendix's Table 3. We believe it best to plot graphs of C_D and C_L vs. spoiler height, with different speeds appearing as different data sets and lines. Because the drag coefficient is not very dependent on wing height, the error bars appear to be extremely large. Nevertheless, the general trend was still visible, i.e., an increase in lift with spoiler height for most speeds (up to a height to chordlength ratio of about 1.3). For the drag coefficients, we saw that the model was, for the average best off without a wing (0.41) and was worst at 0.46 (at a height of 3.3 cm, equivalent to a height to chordlength ratio of 1.3). The instability at spoiler heights of around 2.3 cm (height to chordlength ratio of 1) suggest that this an area of sensitivity. Katz pointed out in Figure 2 that this is approximately the best ratio.

This height, however, was the best height for reducing lift, where the average lift coefficient was actually negative on average, suggesting that significant downforce was generated at this height. At low heights, downforce was negligible, and it seemed that at 3.7 cm (height to chordlength ratio of 1.5), the downforce as indicated by the drag coefficient was beginning to drop. We would have liked to do test at greater heights to see if downforce really does taper off at heights much higher than the roofline, but our apparatus did not allow for it. Furthermore, it would clearly be impractical for every day car use. From looking at the averaged lift coefficients, we see that there is a sudden increase in downforce at 2.6 cm, where the C_L drops from 0.14 to 0.03. However, this is approximately the roofline height. Perhaps those boisterous aftermarket manufacturers really do know what they are doing with very high heights.

Discussion

Our use of a foam interface between the model's wheels and floor were noted earlier. The reason for this is that we could not place the model right onto the floor as the lift forces would then be transferred to the floor rather than the sting. But nor could we let the model be entirely off the ground as we found that the wheels spun in the direction of forward vehicle travel, and preliminary tests showed that this spinning increased lift dramatically. An analogy can be drawn to a rotating cylinder (see Figure 18). Because the relative air speed below the spinning wheel would be lower than that over the wheel, the pressure below the wheel would be greater, generating the witnessed lift. The use of the foam interface effectively stopped the spinning without transferring too much force to the floor. Still, this could be somewhat unrealistic since a travelling vehicle indeed has its wheels spinning. Our neglecting wheel lift would mean a lower than real lift coefficient.



Figure 18: Direction of spinning wheels.

True lift would have its effects first on raising vehicle ride height, and depending on suspension design spring rates, the actual amount of downforce that is reduced may not correspond exactly to the lift generated, but given the minimal suspension travel on the model, it seems that virtually all the lift is transferred to the sting.

We also noticed a difference in lift, and to a lesser extent in drag, by taking away the floor board—slightly higher lift was evident without the floor board. We think that this is because with a floor board, the flow beneath the car has a smaller volume through which to travel. Therefore the flow is accelerated (by the principle of continuity) and the underbody pressure is slightly decreased. This is consistent with high performance cars which tend to be close to the ground to reduce lift effects. Further discussion on "ground effects" is postponed.

We also noted some drifting of the force readouts; an increase in downforce seemed to be typical if one just left the apparatus still at a given speed. As a result, we decided to wait a little while before copying each force reading.

Although the results showed that a higher mounted wing did have more effect in producing downforce with minimal increase in drag, such great heights may not be practical. In terms of safety, they are likely to obstruct rearward vision and may increase manufacturing costs due to the added material to raise the spoiler and the strengthening required to support a higher, more heavily loaded spoiler. If the main factor is truly the height to chordlength ratio, rather than height alone, then a moderately sized rear wing would probably be most effective at moderate heights; since our spoiler was rather large, the optimal heights were also rather high (the most effective, as aforementioned, were 2.6 cm and 3.3 cm).

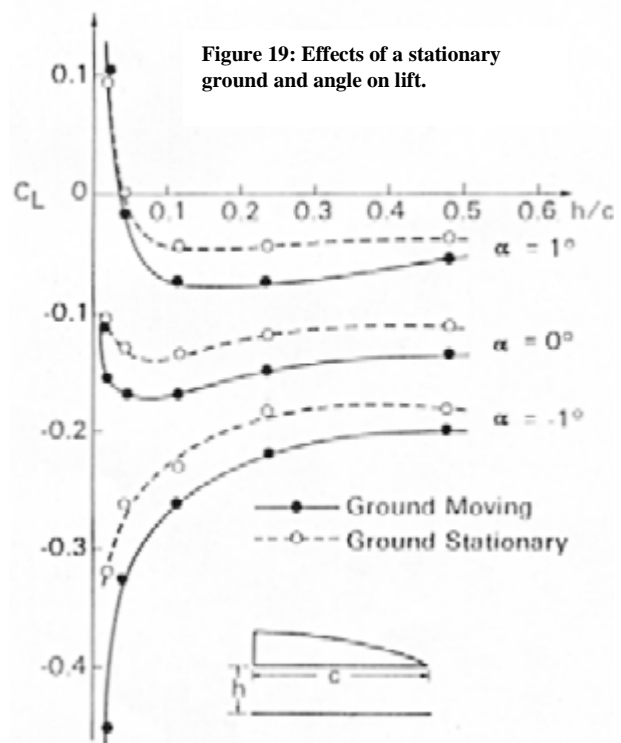
Limitations and Expected Errors from Our Simulation and Experiment Design

While the drag force can be read off the sting quite easily, the lift force cannot be translated as easily into practical terms. Normal aerodynamic testing of vehicles is often quantified by using pressure taps, and therefore the lift imparted on the front and rear axles can be separated, whereas the sting design can only indicate lift at the sting. Because the front of the vehicle is located farther away from the sting, lift there would be magnified due to the increased torque, and the reverse is true for rear end lift. Furthermore, it is impossible to separate the effects of frictional and form drag with our experiment design.

Since our wheels were still rather than moving, we expect that our coefficient values would be underestimated, as a spinning wheel tends to increase drag and lift. Although the foam padding between the tires and the floor did stop the wheels from turning, we think that it might still have transferred some of the forces through to the floor, thereby dampening/underestimating the changes in drag and lift.

We also need to note that our wing has no sides (other than the threaded screws). We expect that a securely mounted wing would show slightly different results due to the existence of the solid supports.

A severe limitation can be found in the fact that, other than in the most complicated wind tunnels, the vehicle remains stationary while the wind blows by, the reverse of real world situations (Hucho (II) 400). A consequence of this is that the relative motion of the wheels with respect to the road and the vehicle become complications, due to differing boundary layer characteristics in the tunnel case and that of a truly moving vehicle. More specifically, with a stationary floor, boundary layer growth along the floor is significant, and the displacement thickness increases along the length of the vehicle, ($d\delta^*/dx$) inducing pressure gradients along the ground itself. Broadly, a wind tunnel ground that is not moving overestimates the real C_L and underestimates the C_D , at least for shapes like vehicles (Bearman 106-09). For example, for a given vehicle-like object with a ground clearance to vehicle length ratio of around 0.07 (typical of a true vehicle), a stationary ground will indicate a C_L of about -0.13, whereas a moving ground would give a value closer to -0.18. A stationary ground tends to decrease the same vehicle's C_D from 0.31 to 0.295. (Bearman 107-09). Thus, one can also see that the inaccuracies of a wind tunnel with a stationary floor produces a greater error in lift than in drag. See Figure 19 above.



The other apparent problem is with the model Viper itself. It is difficult to model all the intricacies of a high performance automobile. We see that many parts of the model that would be sealed in the real car were not, thus allowing flow through the model where it normally would not. As aforementioned, we sealed the windows as best we could to reduce form drag here. The attachment of the sting onto the rear of the vehicle effectively changes the shape of the vehicle and its aerodynamics, and this may be significant since the sting is located where the wakes would normally be.

Perhaps the greatest problem with our experiment is the scale of the model used (1/18). To achieve true dynamic similarity, we would need to test the model at 18 times the road speed, which is clearly not feasible in our wind tunnels. Whereas Reynolds numbers (based on overall length) of vehicles at highway speeds would tend to range from $1 \text{ E}6$ to $1 \text{ E}7$, our 1/18 scale model meant Reynolds numbers ranged from $2.2 \text{ E}5$ to $6.5 \text{ E}5$. At this range, the drag coefficient does not depend exactly on the inverse of the velocity squared, as the lift and drag coefficient equations (Equations 3 and 4) earlier suggested. Instead, the C_D is expected to decrease with increased velocity in our range of Re . In light of this problem, perhaps our 90 mph data would be most accurate as the Re is the highest, and the relative error of the recorded drag and lift forces is smaller. As aforementioned, the 30 mph was somewhat inconsistent. Another consequence of testing in the $1 \text{ E}5$ range for Re is that this order of magnitude is exactly the order of magnitude for transitional flow with low predictability, whereas "[I]n practice, most boundary layers are turbulent...Laminar boundary layers are not common on race cars" (Milliken 97). Perhaps that accounts for our occasional odd data point.

In terms of lift, our low Re testing also has an impact; our tests would generate C_L s that are too high. As the flow, unlike vehicles at highway speeds, is not turbulent and therefore separation and stalling occurs more easily on the wing, reducing its effectiveness in providing downforce.

Conclusions

The results show that the use of rear wings on a passenger vehicle is justified, as the lift coefficient is reduced with the addition of a spoiler. However, there is a marginal increase in the drag coefficient, so an inverted airplane like wing is probably not useful in reducing drag to reduce fuel economy. These propositions will need further testing with better equipment such as a moving floor and a larger scale model to confirm that the results found here hold true on the road at the speeds tested. Our C_L is probably on the high side, due to the stationary floor and low Reynolds number testing, where the latter reduced the wing's efficiency as we cannot confirm that the flow was really turbulent, as in most road cases. Still, the trend that increasing spoiler height to a height to chordlength ratio of around one seems to prove effective in adding a stabilizing downward force.

Acknowledgements

Thanks to Mike Vocaturo for helping us mount the spoiler onto the Viper GTS model.

Thanks to Dr. Felton and Craig Woolsey for answering questions on how our test conditions affect dynamic similarity.

Thanks to Randy Chang for being a very helpful partner.

References [in order referenced in the report]

Smits, A.J. *Lectures in Fluid Mechanics: Introductory Concepts: Volume II*. Unpublished.

Bearman, P.W. "Some Effects of Free-Stream Turbulence and the Presence of the Ground on the Flow Around Bluff Bodies." *Aerodynamic Drag Mechanisms of Bluff Bodies and Road Vehicles*. Eds. Gino Sovran, Thomas Morel and William T. Mason, Jr. New York: Plenum Press, 1978.

Scibor-Rylski, A.J. *Road Vehicle Aerodynamics*. London: Pentech Press, 1975.

Katz, Joseph. *Race Car Aerodynamics: Designing for Speed*. Cambridge: Robert Bentley, 1995.

Hucho, W. – H. "The Aerodynamic of Cars: Current Understanding, Unresolved Problems, and Future prospects." *Aerodynamic Drag Mechanisms of Bluff Bodies and Road Vehicles*. Eds. Gino Sovran, Thomas Morel and William T. Mason, Jr. New York: Plenum Press, 1978.

Wong, J.Y. *Theory of Ground Vehicles*. 2nd ed. New York: John Wiley & Sons, 1993.

Hucho (II), Wolf-Heinrich . *Aerodynamics of Road Vehicles: From Fluid Mechanics to Vehicle Engineering*. Cambridge: Butterworths, 1987.

Milliken, William F., and Douglas L. Milliken. *Race Car Vehicle Dynamics*. Warrendale: SAE International, 1995.

Appendix

Table 2: Aerodynamic data with errors.

Speed (mph)	Speed (m/s)	Spolier Height (cm)	Height: Chordle ngth	Re (car)	Re (model)	Re (wing)	Normal (counts)	Lift (N)	Cl	Axial (counts)	Drag (N)	Cd	Airfoil Length (m)	Chordl ength (cm)	Frontal Area (m ²)															
30	0.5	13.4	0.2	0.0	0.1	0.0	4E+06	2.2E+05	6E+03	2.2E+04	6E+03	-27	1	5.9E-01	0.02	0.88	1.E-01	96	1	3.6E-01	0.00	0.53	2.E-02	1.00E-01	5.E-04	2.55	0.05	6.3E-03	9.E-04	
30	0.5	13.4	0.2	1.5	0.1	0.6	7.E-02	4E+06	2.2E+05	6E+03	2.2E+04	6E+03	1	1	-2.2E-02	0.02	-0.03	3.E-02	86	2	3.2E-01	0.01	0.47	7.E-02	1.00E-01	5.E-04	2.55	0.05	6.3E-03	9.E-04
30	0.5	13.4	0.2	1.9	0.1	0.7	6.E-02	4E+06	2.2E+05	6E+03	2.2E+04	6E+03	-3	5	6.5E-02	0.11	0.10	2.E-01	92	3	3.4E-01	0.01	0.51	8.E-02	1.00E-01	5.E-04	2.55	0.05	6.3E-03	9.E-04
30	0.5	13.4	0.2	2.3	0.1	0.9	5.E-02	4E+06	2.2E+05	6E+03	2.2E+04	6E+03	-4	2	8.7E-02	0.04	0.13	7.E-02	82	2	3.0E-01	0.01	0.45	7.E-02	1.00E-01	5.E-04	2.55	0.05	6.3E-03	9.E-04
30	0.5	13.4	0.2	2.6	0.1	1.0	4.E-02	4E+06	2.2E+05	6E+03	2.2E+04	6E+03	6	1	-1.3E-01	0.02	-0.19	4.E-02	100	2	3.7E-01	0.01	0.55	9.E-02	1.00E-01	5.E-04	2.55	0.05	6.3E-03	9.E-04
30	0.5	13.4	0.2	3.3	0.1	1.3	4.E-02	4E+06	2.2E+05	6E+03	2.2E+04	6E+03	14	2	-3.1E-01	0.04	-0.45	1.E-01	93	2	3.4E-01	0.01	0.51	8.E-02	1.00E-01	5.E-04	2.55	0.05	6.3E-03	9.E-04
30	0.5	13.4	0.2	3.7	0.1	1.5	3.E-02	4E+06	2.2E+05	6E+03	2.2E+04	6E+03	8	1	-1.7E-01	0.02	-0.26	5.E-02	95	3	3.5E-01	0.01	0.52	8.E-02	1.00E-01	5.E-04	2.55	0.05	6.3E-03	9.E-04
50	0.5	22.4	0.2	0.0	0.1	0.0	6E+06	3.6E+05	8E+03	3.7E+04	9E+03	-36	1	7.8E-01	0.02	0.42	6.E-02	203	3	7.5E-01	0.01	0.40	6.E-02	1.00E-01	5.E-04	2.55	0.05	6.3E-03	9.E-04	
50	0.5	22.4	0.2	1.5	0.1	0.6	7.E-02	6E+06	3.6E+05	8E+03	3.7E+04	9E+03	-10	1	2.2E-01	0.02	0.12	2.E-02	208	4	7.7E-01	0.01	0.41	6.E-02	1.00E-01	5.E-04	2.55	0.05	6.3E-03	9.E-04
50	0.5	22.4	0.2	1.9	0.1	0.7	6.E-02	6E+06	3.6E+05	8E+03	3.7E+04	9E+03	-13	2	2.8E-01	0.04	0.15	3.E-02	214	5	7.9E-01	0.02	0.42	7.E-02	1.00E-01	5.E-04	2.55	0.05	6.3E-03	9.E-04
50	0.5	22.4	0.2	2.3	0.1	0.9	5.E-02	6E+06	3.6E+05	8E+03	3.7E+04	9E+03	-8	1	1.7E-01	0.02	0.09	2.E-02	212	5	7.8E-01	0.02	0.42	6.E-02	1.00E-01	5.E-04	2.55	0.05	6.3E-03	9.E-04
50	0.5	22.4	0.2	2.6	0.1	1.0	4.E-02	6E+06	3.6E+05	8E+03	3.7E+04	9E+03	-2	1	4.4E-02	0.02	0.02	1.E-02	220	5	8.1E-01	0.02	0.44	7.E-02	1.00E-01	5.E-04	2.55	0.05	6.3E-03	9.E-04
50	0.5	22.4	0.2	3.3	0.1	1.3	4.E-02	6E+06	3.6E+05	8E+03	3.7E+04	9E+03	9	2	-2.0E-01	0.04	-0.11	3.E-02	224	3	8.3E-01	0.01	0.44	7.E-02	1.00E-01	5.E-04	2.55	0.05	6.3E-03	9.E-04
50	0.5	22.4	0.2	3.7	0.1	1.5	3.E-02	6E+06	3.6E+05	8E+03	3.7E+04	9E+03	4	1	-8.7E-02	0.02	-0.05	1.E-02	217	3	8.0E-01	0.01	0.43	7.E-02	1.00E-01	5.E-04	2.55	0.05	6.3E-03	9.E-04
60	0.5	26.8	0.2	0.0	0.1	0.0	8E+06	4.3E+05	9E+03	4.5E+04	1.E+04	-42	2	9.2E-01	0.04	0.34	5.E-02	285	5	1.1E+00	0.02	0.39	6.E-02	1.00E-01	5.E-04	2.55	0.05	6.3E-03	9.E-04	
60	0.5	26.8	0.2	1.5	0.1	0.6	7.E-02	8E+06	4.3E+05	9E+03	4.5E+04	1.E+04	-19	1	4.1E-01	0.02	0.15	2.E-02	303	7	1.1E+00	0.03	0.42	6.E-02	1.00E-01	5.E-04	2.55	0.05	6.3E-03	9.E-04
60	0.5	26.8	0.2	1.9	0.1	0.7	6.E-02	8E+06	4.3E+05	9E+03	4.5E+04	1.E+04	-18	2	3.9E-01	0.04	0.15	3.E-02	305	5	1.1E+00	0.02	0.42	6.E-02	1.00E-01	5.E-04	2.55	0.05	6.3E-03	9.E-04
60	0.5	26.8	0.2	2.3	0.1	0.9	5.E-02	8E+06	4.3E+05	9E+03	4.5E+04	1.E+04	-17	3	1.3E-01	0.07	0.14	3.E-02	330	10	1.2E+00	0.04	0.45	7.E-02	1.00E-01	5.E-04	2.55	0.05	6.3E-03	9.E-04
60	0.5	26.8	0.2	2.6	0.1	1.0	4.E-02	8E+06	4.3E+05	9E+03	4.5E+04	1.E+04	-6	1	1.3E-01	0.02	0.05	1.E-02	310	10	1.1E+00	0.04	0.43	7.E-02	1.00E-01	5.E-04	2.55	0.05	6.3E-03	9.E-04
60	0.5	26.8	0.2	3.3	0.1	1.3	4.E-02	8E+06	4.3E+05	9E+03	4.5E+04	1.E+04	-4	1	8.7E-02	0.02	0.03	9.E-03	330	8	1.2E+00	0.03	0.45	7.E-02	1.00E-01	5.E-04	2.55	0.05	6.3E-03	9.E-04
60	0.5	26.8	0.2	3.7	0.1	1.5	3.E-02	8E+06	4.3E+05	9E+03	4.5E+04	1.E+04	-5	1	1.1E-01	0.02	0.04	1.E-02	325	5	1.2E+00	0.02	0.45	7.E-02	1.00E-01	5.E-04	2.55	0.05	6.3E-03	9.E-04
70	1	31.3	0.4	0.0	0.1	0.0	9E+06	5.0E+05	1.E+04	5.2E+04	1.E+04	-32	2	7.0E-01	0.04	0.19	3.E-02	370	10	1.4E+00	0.04	0.37	6.E-02	1.00E-01	5.E-04	2.55	0.05	6.3E-03	9.E-04	
70	1	31.3	0.4	1.5	0.1	0.6	7.E-02	9E+06	5.0E+05	1.E+04	5.2E+04	1.E+04	-29	1	6.3E-01	0.02	0.17	3.E-02	410	10	1.5E+00	0.04	0.40	6.E-02	1.00E-01	5.E-04	2.55	0.05	6.3E-03	9.E-04
70	1	31.3	0.4	1.9	0.1	0.7	6.E-02	9E+06	5.0E+05	1.E+04	5.2E+04	1.E+04	-26	3	5.7E-01	0.07	0.16	3.E-02	400	10	1.5E+00	0.04	0.42	6.E-02	1.00E-01	5.E-04	2.55	0.05	6.3E-03	9.E-04
70	1	31.3	0.4	2.3	0.1	0.9	5.E-02	9E+06	5.0E+05	1.E+04	5.2E+04	1.E+04	-23	2	5.0E-01	0.04	0.14	2.E-02	433	10	1.6E+00	0.04	0.44	7.E-02	1.00E-01	5.E-04	2.55	0.05	6.3E-03	9.E-04
70	1	31.3	0.4	2.6	0.1	1.0	4.E-02	9E+06	5.0E+05	1.E+04	5.2E+04	1.E+04	-9	1	2.0E-01	0.02	0.05	1.E-02	430	10	1.6E+00	0.04	0.44	7.E-02	1.00E-01	5.E-04	2.55	0.05	6.3E-03	9.E-04
70	1	31.3	0.4	3.3	0.1	1.3	4.E-02	9E+06	5.0E+05	1.E+04	5.2E+04	1.E+04	-16	2	3.5E-01	0.04	0.10	2.E-02	440	9	1.6E+00	0.03	0.45	7.E-02	1.00E-01	5.E-04	2.55	0.05	6.3E-03	9.E-04
70	1	31.3	0.4	3.7	0.1	1.5	3.E-02	9E+06	5.0E+05	1.E+04	5.2E+04	1.E+04	-7	2	1.5E-01	0.04	0.04	1.E-02	430	10	1.6E+00	0.04	0.44	7.E-02	1.00E-01	5.E-04	2.55	0.05	6.3E-03	9.E-04
90	1	40.2	0.4	0.0	0.1	0.0	1E+07	6.5E+05	1.E+04	6.7E+04	2.E+04	-117	3	2.6E+00	0.07	0.42	6.E-02	590	10	2.2E+00	0.04	0.36	6.E-02	1.00E-01	5.E-04	2.55	0.05	6.3E-03	9.E-04	
90	1	40.2	0.4	1.5	0.1	0.6	7.E-02	1E+07	6.5E+05	1.E+04	6.7E+04	2.E+04	-123	2	2.7E+00	0.04	0.44	7.E-02	645	15	2.4E+00	0.06	0.39	6.E-02	1.00E-01	5.E-04	2.55	0.05	6.3E-03	9.E-04
90	1	40.2	0.4	1.9	0.1	0.7	6.E-02	1E+07	6.5E+05	1.E+04	6.7E+04	2.E+04	-73	3	1.6E+00	0.07	0.26	4.E-02	670	20	2.5E+00	0.07	0.41	6.E-02	1.00E-01	5.E-04	2.55	0.05	6.3E-03	9.E-04
90	1	40.2	0.4	2.3	0.1	0.9	5.E-02	1E+07	6.5E+05	1.E+04	6.7E+04	2.E+04	-56	3	1.2E+00	0.07	0.20	3.E-02	710	20	2.6E+00	0.07	0.43	7.E-02	1.00E-01	5.E-04	2.55	0.05	6.3E-03	9.E-04
90	1	40.2	0.4	2.6	0.1	1.0	4.E-02	1E+07	6.5E+05	1.E+04	6.7E+04	2.E+04	-55	2	1.2E+00	0.04	0.20	3.E-02	680	10	2.5E+00	0.04	0.42	6.E-02	1.00E-01	5.E-04	2.55	0.05	6.3E-03	9.E-04
90	1	40.2	0.4	3.3	0.1	1.3	4.E-02	1E+07	6.5E+05	1.E+04	6.7E+04	2.E+04	-82	3	1.8E+00	0.07	0.30	5.E-02	705	10	2.6E+00	0.04	0.43	7.E-02	1.00E-01	5.E-04	2.55	0.05	6.3E-03	9.E-04
90	1	40.2	0.4	3.7	0.1	1.5	3.E-02	1E+07	6.5E+05	1.E+04	6.7E+04	2.E+04	-77	3	1.7E+00	0.07	0.28	4.E-02	685	15	2.5E+00	0.06	0.42	6.E-02	1.00E-01	5.E-04	2.55	0.05	6.3E-03	9.E-04

Table 3: Data based on spoiler height with average coefficients.

Speed (mph)	Spolier Height (cm)	Height: Chordle ngth	Re (car)	Re (model)	Re (wing)	Cl	Cd	Cl avg.	Cd avg.
30	0.0	0.0	4E+06	2.2E+05	2.2E+04	0.88	0.53	0.45	0.41
50	0.0	0.0	6E+06	3.6E+05	3.7E+04	0.42	0.40		
60	0.0	0.0	8E+06	4.3E+05	4.5E+04	0.34	0.39		
70	0.0	0.0	9E+06	5.0E+05	5.2E+04	0.19	0.37		
90	0.0	0.0	1E+07	6.5E+05	6.7E+04	0.42	0.36		
30	1.5	0.6	4E+06	2.2E+05	2.2E+04	-0.03	0.47	0.17	0.42
50	1.5	0.6	6E+06	3.6E+05	3.7E+04	0.12	0.41		
60	1.5	0.6	8E+06	4.3E+05	4.5E+04	0.15	0.42		
70	1.5	0.6	9E+06	5.0E+05	5.2E+04	0.17	0.40		
90	1.5	0.6	1E+07	6.5E+05	6.7E+04	0.44	0.39		
30	1.9	0.7	4E+06	2.2E+05	2.2E+04	0.10	0.51	0.16	0.44
50	1.9	0.7	6E+06	3.6E+05	3.7E+04	0.15	0.42		
60	1.9	0.7	8E+06	4.3E+05	4.5E+04	0.15	0.42		
70	1.9	0.7	9E+06	5.0E+05	5.2E+04	0.16	0.42		
90	1.9	0.7	1E+07	6.5E+05	6.7E+04	0.26	0.41		
30	2.3	0.9	4E+06	2.2E+05	2.2E+04	0.13	0.45	0.14	0.44
50	2.3	0.9	6E+06	3.6E+05	3.7E+04	0.09	0.42		
60									

Table 4: Sting calibration data.

Angle (°)	Mass (kg)	Weight (N)	Normal Force (counts)	Normal Force (N)	Axial Force (counts)	Axial Force (N)
0	0.00E+00	0.00	0	0.00E+00		
0	2.00E-02	0.20	8	1.96E-01		
0	5.00E-02	0.49	22	4.90E-01		
0	1.00E-01	0.98	45	9.80E-01		
0	2.00E-01	1.96	90	1.96E+00		
0	5.00E-01	4.90	225	4.90E+00		
15	0.00E+00	0.00			0	0.00E+00
15	2.00E-02	0.20			-73	-5.07E-02
15	5.00E-02	0.49			-87	-1.27E-01
15	1.00E-01	0.98			-114	-2.54E-01
15	2.00E-01	1.96			-158	-5.07E-01
15	5.00E-01	4.90			-288	-1.27E+00

Equation 8: Calculation of model frontal area.

$$A_f = 1.6 + 0.00056(m_v - 765)$$

$$A_f = 1.6 + 0.00056(1550 - 765)$$

$$A_{f_{real}} = 2.0396m^2$$

$$A_{f_{model}} = 0.0063m^2$$

Figure 20: **Sting Calibration Chart**

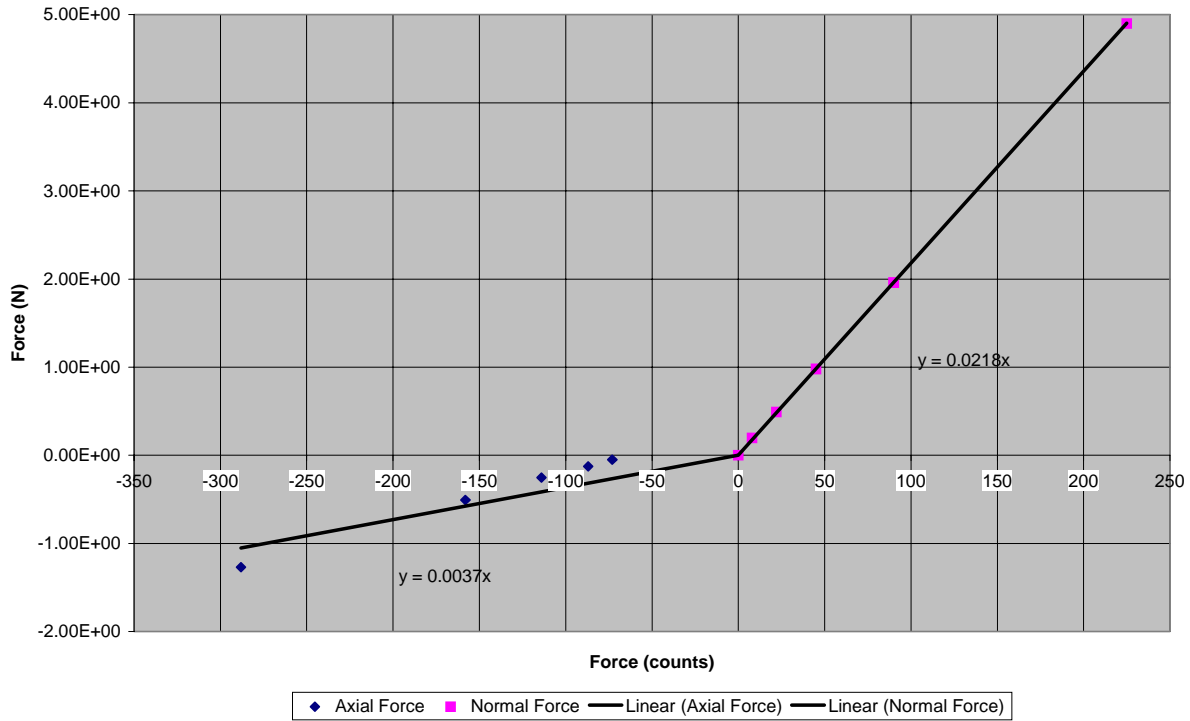


Table 5: Ambient Data.

	Pressure (cm HG)	Pressure (psi)	Pressure (Pa)	Temperature (°C)	Temperature (K)	R (J/kgK)	ρ (kg/m ³)
Recorded	75.50	14.60	1.01E+05	19.0	292	291	1.185E+00
δ	0.05	0.01	67	0.5	0.5		2.17E-03
$\partial p / \partial p$			1.18E-05				
$\partial p / \partial T$					-4.06E-03		